

Some Properties of Radio Galaxies in Clusters

O. B. Slee,^A *I. R. G. Wilson*^B and *Betty C. Siegman*^A

^A Division of Radiophysics, CSIRO, P.O. Box 76, Epping, N.S.W. 2121.

^B Mount Stromlo and Siding Spring Observatories, Private Bag, Woden, A.C.T. 2606.

Abstract

We present a statistical survey of the properties of 148 radio sources that are highly likely to be in Abell clusters, and compare them with 127 identified field sources with the same range of redshifts from the Culgoora-3 list.

We show that: (i) the sources are highly concentrated towards the cluster centres; (ii) the probability of finding a source in a cluster is independent of cluster richness; (iii) the sources occur relatively much more frequently in Bautz–Morgan (B–M) I clusters; (iv) the spectral index is not dependent on cluster richness but increases towards the cluster centres and is highest in clusters of morphological class B–M I; (v) the radio power $P_{1.60}$ is highest for sources within 0.10 Abell radius of cluster centres but does not depend on a cluster's richness or its optical morphology; the linear sizes of radio galaxies do not depend upon cluster richness, distance from the cluster centre or optical morphology.

A comparison of the properties of sources in clusters with those of the Culgoora-3 field sample shows: (i) the spectral indices of cluster sources are higher than spectral indices of field sources, particularly if the cluster sources are near cluster centres and/or in B–M I clusters; (ii) there is significant second-degree and third-degree curvature in the spectra of both cluster and field sources but the curvature is more pronounced in the cluster sample; (iii) the sources in clusters are not particularly powerful, i.e. field sources emit a median $P_{1.60}$ which is ~ 4 times that of cluster sources; (iv) the cluster sources have a median overall linear dimension that is ~ 130 kpc smaller than that of the field sources, a decrease which is *not* due to the lower power of cluster sources; (v) the luminosity functions for both cluster and field sources have a power-law form and possess very similar power-law exponents, only about 20% of radio galaxies with $0.02 < z < 0.20$ being located in rich clusters.

Our results support the hypothesis that the spectra and dimensions of radio sources in clusters are influenced by a hot, relatively dense electron gas and that radio observations are more sensitive detectors of this gas than are existing optical or X-ray studies.

1. Introduction

There has been a number of general radio surveys of clusters of galaxies made by various observers during the last 18 years: Pilkington (1964), Wills (1966), Komesaroff *et al.* (1968), Owen (1974, 1975) and Mills and Hoskins (1977). In addition specific surveys at low frequencies have been made of the stronger X-ray emitting clusters by Erickson *et al.* (1978), Slee and Quinn (1979) and Dagkesamansky *et al.* (1982). These investigations have attempted to answer such questions as: (i) How strongly are radio galaxies concentrated towards the cluster centre? (ii) Are the spectral indices of radio galaxies in clusters different from those of field radio galaxies?

(iii) What is the radio luminosity function of cluster radio galaxies? (iv) How does cluster richness and optical morphology influence the above properties? (v) Does cluster membership influence the linear dimensions of a radio galaxy? (vi) What kinds of optical galaxies are identified with cluster radio sources?

In this paper we present a statistical analysis of the first five of these topics. We believe that the results are based on the most comprehensive data yet gathered. In Section 2 we describe the data base and criteria for selecting radio sources for cluster membership. Sections 3, 4, 5 and 6 are concerned with the influences of cluster parameters on source distributions, radio spectral index, radio power and radio linear dimensions respectively. Section 7 summarizes the differences in radio properties between cluster and field radio galaxies, while Section 8 describes how the radio, X-ray and optical observations of clusters can be related and used in order to derive some qualitative conclusions about the physical conditions in clusters.

2. Data Base

The present investigation stems from two observational programs that the authors conducted between 1978 and 1981: (i) measurements with the Culgoora circular array (CCA) at 80 and 160 MHz of the flux densities and angular sizes of 367 sources near 246 Abell (1958) clusters that had been partly surveyed by Mills and Hoskins (1977) and Owen (1974, 1975); (ii) a survey at 2700 MHz with the Parkes 64 m reflector out to 1.5 Abell radii of 80 Abell clusters including all 55 clusters out to distance class 4 in Abell's complete statistical sample with declinations south of $+20^\circ$. Papers giving the full results of these observational programs are in preparation. A preliminary analysis of the spectral indices of sources in the CCA cluster sample was given by Slee *et al.* (1982*b*).

We have used the Parkes 2700 MHz survey to establish the degree of concentration of radio sources towards the cluster centres. Fig. 1*a* shows the counts in equal area bins for sources in 76 Abell clusters of distance classes 3 and 4; we have included only sources with $S_{2700} \geq 0.12$ Jy, which we estimate to be the completeness level of our survey. This plot includes all surveyed clusters of distance classes 3 and 4, but a similar plot is obtained for the 55 clusters in Abell's complete sample.

It is clear from Fig. 1*a* that the source density rises significantly above the expected background level of sources [deduced from a deep 2700 MHz survey by Wall *et al.* (1971)] in the central annular bin of 0.40 Abell radius; here the mean source density is ~ 3.5 times the background. The sources in this bin are further allocated to smaller equal-area bins in Fig. 1*b*, which clearly shows that the source density in the central 0.20 Abell radius bin is about eight times the expected background source density. These 2700 MHz distributions are similar to those found in analyses of 178 MHz sources from the 4C survey by Pilkington (1964), Wills (1966) and McHardy (1979), the latter author giving a source density of 22 times the 178 MHz background density within 0.10 Abell radius. The conclusion is that there can be no important difference in the radio source populations of Abell clusters at these widely different frequencies: in particular there can be no significant concentration of flat-spectrum sources in clusters; 89% of the 2700 MHz sources in the central bin of Fig. 1*a* were detected in our 80/160 MHz observations and (considering the flux limits of the observations) the 11% of undetected sources could have possessed spectral indices as high as -0.91 .

The cluster sources selected for observation with the CCA at 80 and 160 MHz were chosen from five surveys of clusters: (i) sources from Owen (1974) with $S_{1400} \geq 0.2$ Jy

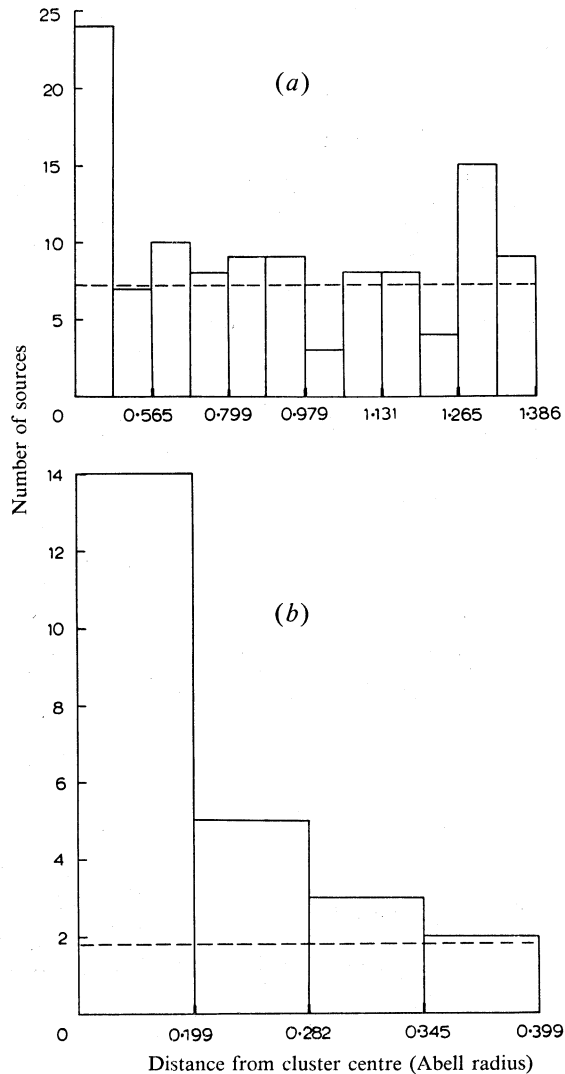


Fig. 1. Distributions of radio sources in our Parkes 11 cm survey of a complete sample of Abell clusters with distance from the cluster centre. The bins are of equal solid angle and the dashed horizontal line represents an estimate of the background source density from an 11 cm survey by Wall *et al.* (1971); see text for further details. Parts (a) and (b) refer to successively finer subdivisions of the distance scale.

and declinations south of $+35^\circ$, this survey being complete out to ~ 0.6 Abell radius; (ii) sources from Owen (1975) with $S_{2695} \geq 0.10$ Jy and south of $+35^\circ$, this survey also being complete to ~ 0.6 Abell radius; (iii) all sources in the Mills and Hoskins (1977) 408 MHz survey of 247 Abell clusters south of declination $+18^\circ$, which extends out to at least the Abell radius; (iv) all sources with $S_{2700} \geq 0.06$ Jy from the present Parkes survey of 80 clusters south of $+20^\circ$; this survey extends out

to 1.5 Abell radii, but we observed with the CCA only those sources within 1.10 Abell radii; (v) an unpublished survey at 80 MHz with the CCA of all 130 clusters south of $+35^\circ$ with distance 5, richness ≥ 2 and distance 6, richness ≥ 3 , this survey extending out to 0.5 Abell radius. In summary, a total of 257 sources were detected in 640 Abell clusters, the sources being derived from surveys that were complete out to at least 0.50 Abell radius. The flux density limits of our CCA measurements ($5 \times$ r.m.s.) were ~ 3.0 Jy per beam at 80 MHz and ~ 2.0 Jy per beam at 160 MHz. Contour maps were constructed at 160 MHz of 134 sources, 118 of which were significantly resolved by the $1'.9$ arc beam in at least one direction; two-dimensional elliptical gaussians were computer fitted to the resolved sources, the resulting major axes of the ellipses being used to estimate the maximum linear dimensions of cluster sources. The methods used for the making of maps, fitting the brightness distributions and computation of linear power-law spectra for these sources were the same as those used by Slee *et al.* (1982a) in analysing the Culgoora-3 list of sources (Slee 1977).

The information from our 2700 MHz survey in Fig. 1 was used to establish a criterion for cluster membership: all sources in the CCA measurements situated within 0.40 Abell radius of a cluster centre were accepted as cluster members, but only the 148 sources which had been observed at ≥ 3 widely spaced frequencies between 80 MHz and 5 GHz were included in our final statistical sample; this precaution was needed to establish acceptable radio spectra.

Table 1. Median parameters of the CCA sample

Distance class	No. of sources	Median redshift ^A	Median S_{160} (Jy)	Median angular size ^B (' arc)
1 & 2	15	0.026	4.7	2.9 (8)
3	32	0.055	2.3	2.3 (14)
4	31	0.076	2.7	3.2 (19)
5	49	0.126	2.8	2.4 (26)
6	25	0.169	2.6	2.0 (12)

^A From the m_{10}/z relationship of Mills and Hoskins (1977).

^B Major axis to half-brightness of the elliptical gaussian with the best fit to contours; the number of resolved sources in each distance class is in parentheses.

Table 1 shows the median observed parameters of the CCA sample of sources in clusters; it is clear that the observed flux densities and angular sizes show little dependence on the distances (redshifts) of the associated clusters. This implies that we sample increasingly more powerful and larger radio galaxies as the cluster distances increase and that there should be significant correlations between computed radio power P_{160} and redshift z and between linear size L_{kpc} and redshift z . There are indeed such correlations, and we have used power-law fits to all the P_{160}/z and L_{kpc}/z data in the sample to derive expressions for correcting these quantities to a standard redshift of $z = 0.100$; such a procedure is necessary in deriving the dependences of P_{160} and L_{kpc} on cluster parameters. All our computations of P_{160} and L_{kpc} make use of a Hubble constant $H_0 = 50 \text{ km s}^{-1} \text{ Mpc}^{-1}$ and an Einstein-de Sitter cosmology. We have investigated the data for a correlation between spectral index and redshift α/z of the kind described by Slee (1981) for the Culgoora-3 sample of sources. No

α/z relationship can be found in the CCA cluster sample; if such a relationship exists it cannot be detected because of the strong influences associated with the clusters themselves.

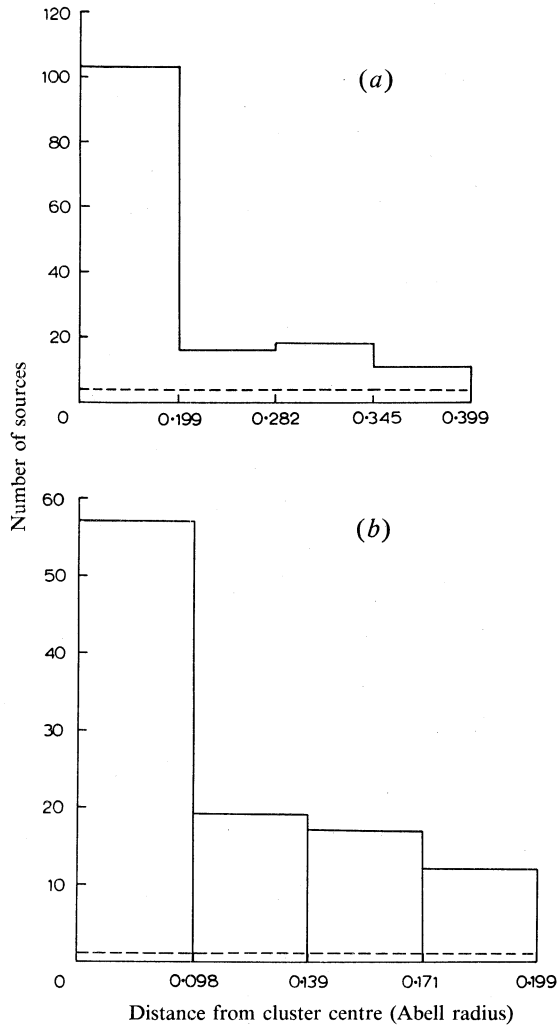


Fig. 2. Distributions of radio sources in the CCA sample with distance from the cluster centre. The bins are of equal solid angle and the dashed horizontal line represents an estimate of the background source density from Gower's (1966) analysis of the 4C survey. Parts (a) and (b) refer to successively finer subdivisions of the distance scale.

Most of the conclusions of this paper are based on statistical analyses of the distributions of spectral index α , emitted 160 MHz power P_{160} and linear size L_{kpc} . When a distribution approximated the normal distribution (e.g. α) we gave preference to parametric tests of significance of the differences between means (the 't' statistic) and Fisher's F-test in analysis of variance; in all cases however we checked the result by

using a distribution-free statistic, namely the Kruskal–Wallis ranking test for two or more independent groups (Hughes and Grawoig 1971). In testing distributions such as those for P_{160} and L_{kpc} , which display a marked degree of asymmetry, the computation of medians together with the use of the K–W ranking test was considered to be essential.

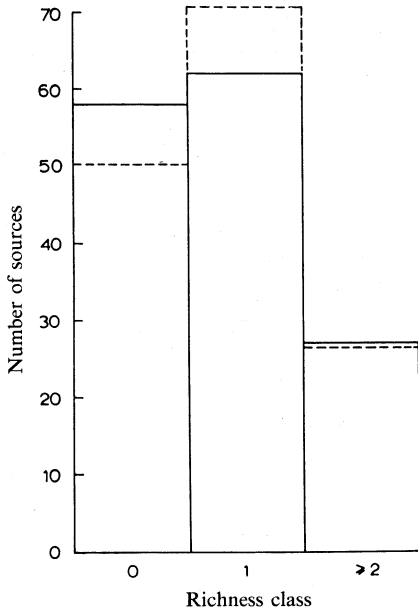


Fig. 3. Distribution of sources in the CCA sample with respect to Abell's richness classes. The dashed outline gives the numbers of sources expected if they were distributed equally among Abell's richness classes.

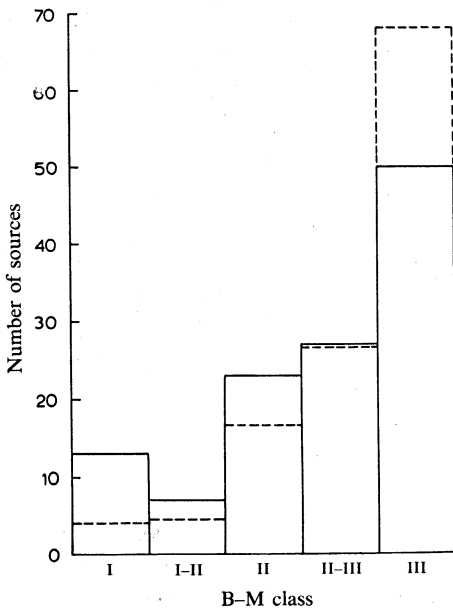


Fig. 4. Distribution of CCA sources with respect to the Bautz–Morgan (B–M) classifications of optical morphology. The dashed outline shows the numbers of sources expected if they were distributed equally among the various B–M classes.

3. Distributions for Cluster Sources

Variation with Distance from Cluster Centre

Fig. 2 shows the numbers of CCA sources in bins of equal solid angle out to distances of (a) 0.40 and (b) 0.20 Abell radius. The dashed line on each distribution is our estimate of the background source count at 160 MHz; this was obtained by summing the solid angles subtended by circles of the appropriate radius in all 640 surveyed clusters and multiplying this figure by a background source density of $1000 \text{ sources sr}^{-1}$ from the 4C survey at 178 MHz (Gower 1966), which is appropriate to the lowest flux density of $S_{160} = 1.6 \text{ Jy}$ measured for this sample. It is clear that the CCA distributions are similar to those from our 11 cm survey in Fig. 1. We note the very marked increase in cluster sources within 0.20 Abell radius of the cluster centres.

Variation with Cluster Richness

Fig. 3 gives the distribution of CCA cluster sources in three increments of cluster richness. The number of radio galaxies in each richness class is not significantly different from the expected number (dashed line) computed from the fraction of clusters in that richness class from Abell's catalogue. Fig. 3 means, in effect, that one is just as likely to detect a radio galaxy in a poor cluster as in a rich cluster, agreeing with the conclusions of Mills and Hoskins (1977) and McHardy (1979) on the same subject.

Variation with Optical Morphology

Fig. 4 shows the distribution of CCA cluster sources with B-M classes of optical morphology. The dashed line in each bin represents the count expected from the relative frequencies of occurrence given by Leir and van den Bergh (1977). A χ^2 test shows that the observed and expected distributions differ very significantly in that more than three times as many sources as expected are seen in B-M I clusters. Thus, the presence of a dominant cD galaxy near the cluster centre (the criterion for B-M I classification) increases significantly the probability of strong radio emission. This agrees with McHardy's (1979) analysis of 4C sources associated with clusters.

Distance from Cluster Centre and Optical Morphology

We show in Fig. 5 how the distances of CCA sources from their cluster centres depend upon the optical morphologies of their associated clusters. An analysis of variance within and between the four B-M classes (Fisher's F-test), together with the K-W ranking test, supports the hypothesis that the distances of sources from cluster centres are independent of B-M class.

Summarizing this section on source distributions we find that: (i) the sources are strongly concentrated to within 0.2 Abell radius of the cluster centre; (ii) the probability of finding a source in a cluster is independent of cluster richness; (iii) the sources occur relatively much more frequently in B-M I clusters; and (iv) the distances of sources from cluster centres are independent of cluster optical morphology.

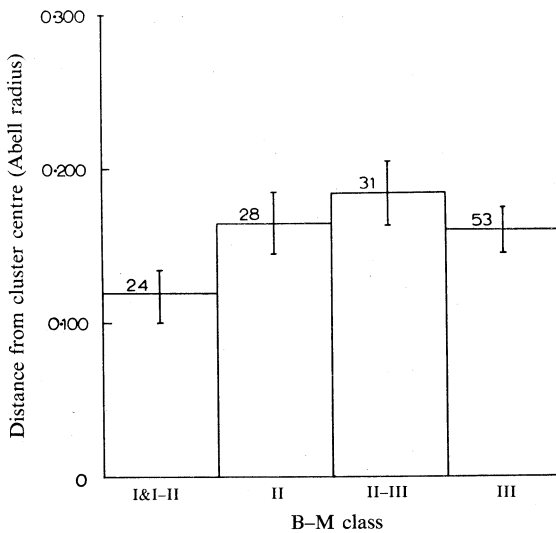


Fig. 5. Diagram showing how the sources in the CCA cluster sample are distributed both with respect to the optical morphology of the clusters and with respect to distance from the cluster centre. The number of sources in each bin together with the standard error of their mean distance is shown.

4. Spectral Indices of Cluster Sources

Variation of Spectral Index with Distance from Cluster Centre

Fig. 6a shows that the spectral index of CCA cluster sources is highest near the centre of a cluster. An analysis of variance (F-test) supported by the K-W ranking test shows that the three samples are unlikely to have been drawn from a common population ($p = 0.05$). Computation of the linear regression of spectral index α on distance from cluster centre r/R_A , where R_A is the Abell radius, gives a regression equation:

$$|\alpha| = 0.953 - 0.524 r/R_A.$$

The correlation coefficient is 0.215, which is significant at $p = 0.02$. A small part of the decrease in spectral index may be due to the inclusion of more background sources with increasing angular distance from the cluster centre; however Fig. 2a shows that only ~20% of the total number of sources between 0.20 and 0.40 Abell radius can be in this category, and accordingly their influence on the average spectral index is not important.

Spectral Index and Cluster Richness

The dependence of spectral index on cluster richness is shown in Fig. 6b. While the spectral index *appears* to increase with richness, an analysis of variance and a ranking test fail to show that the indices have been drawn from different populations. McHardy's (1979) analysis of 4C cluster sources showed an increase of index with richness, but his sample contained less than one-third of the number of radio sources in our CCA sample.

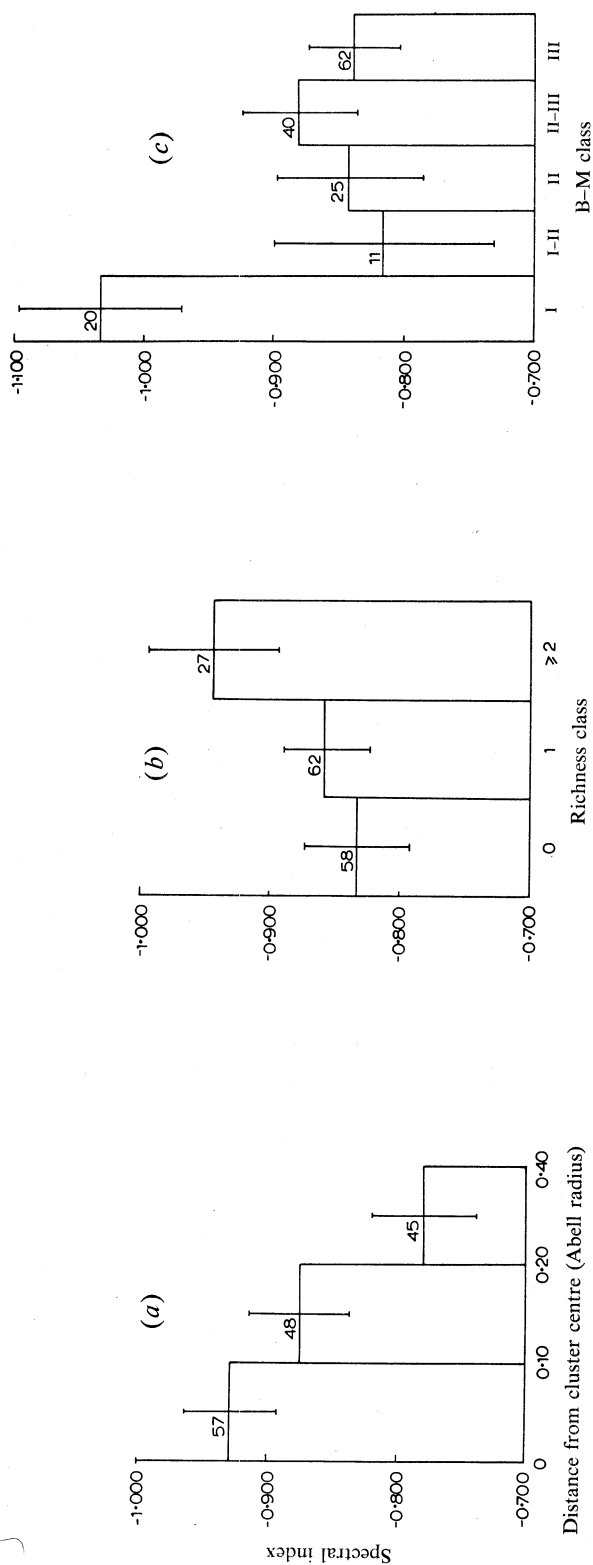


Fig. 6. Variation of spectral index with (a) distance from the cluster centre, (b) Abell's richness class and (c) the optical morphology of the cluster. The number of sources in each mean spectral index together with its standard error is shown.

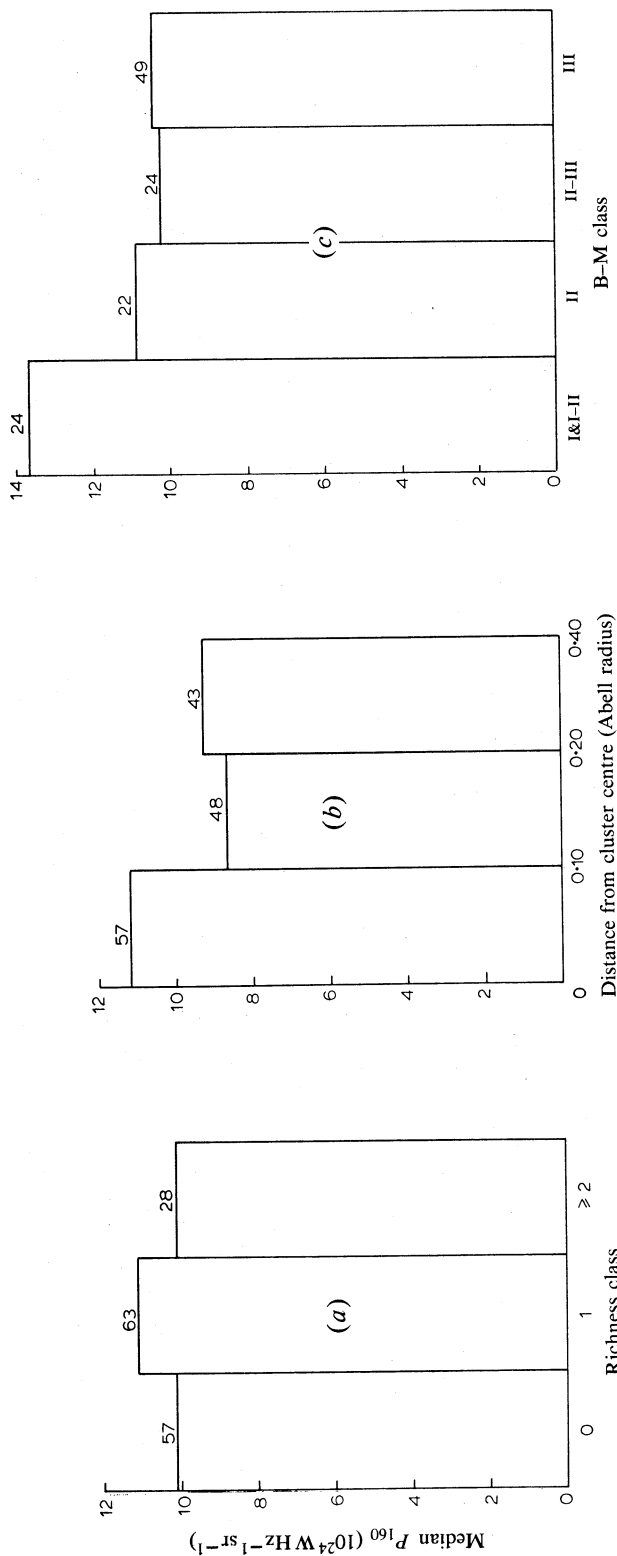


Fig. 7. Relationship between the median 160 MHz power emitted by sources in the CCA cluster sample and (a) Abell's richness class, (b) their distances from the cluster centre and (c) the optical morphology of the clusters. The number of sources in each class or interval is shown.

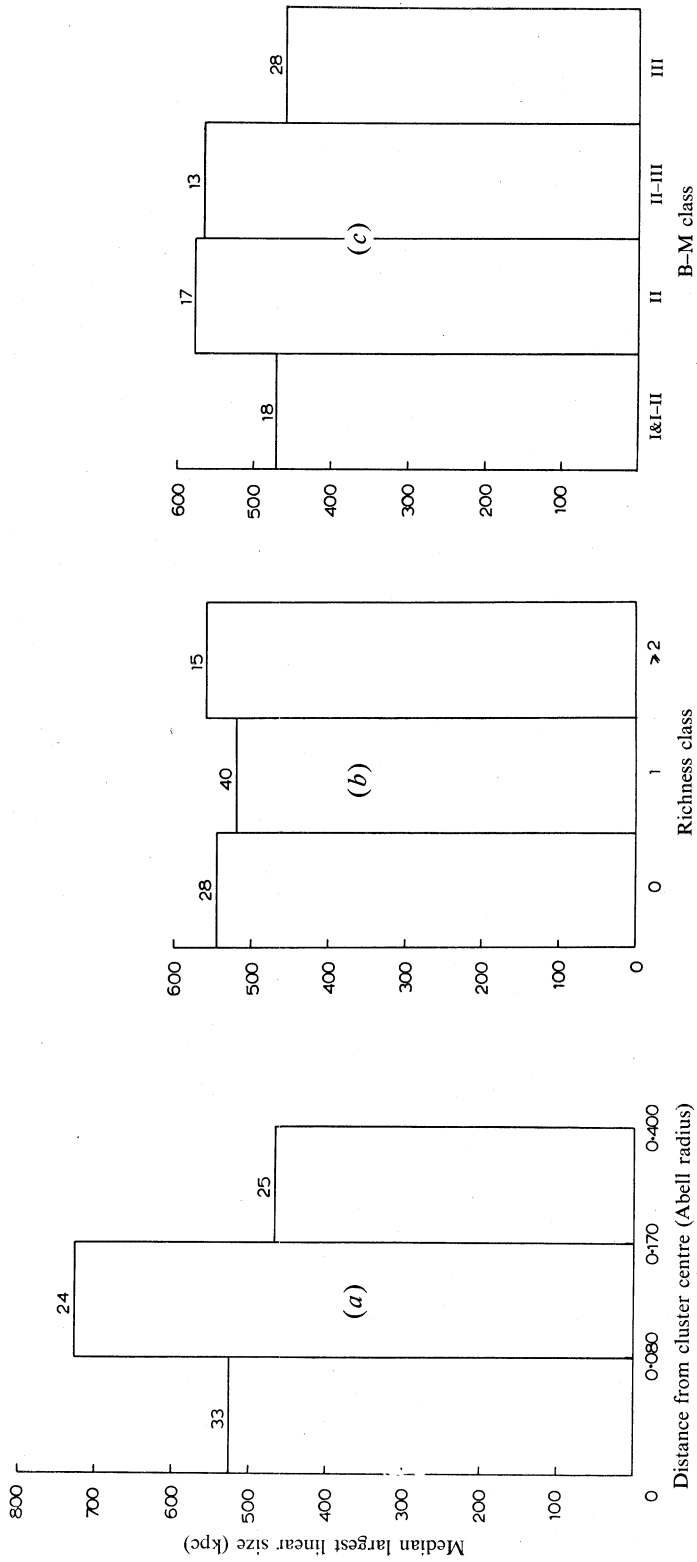


Fig. 8. Dependence of median linear sizes of the resolved sources in the CCA cluster sample on (a) their distance from the cluster centre, (b) Abell's richness class and (c) the B-M morphological class. (See Section 6 for our definition of the largest linear size.) The number of sources in each interval or class is shown.

Dependence of Spectral Index on Optical Morphology

Fig. 6c shows the influence of cluster morphology on the spectral indices of CCA sources. An analysis of variance and a ranking test indicate that there is a probability of $p = 0.06$ that the five samples could have been drawn by chance from the same population. Testing the B–M I sample against the combination of all other B–M classes (bearing in mind that there are six possible ways of choosing such a combination), we find that the difference between the two distributions is significant at $p = 0.03$. There is little doubt that sources in B–M I clusters have much higher spectral indices than those in later morphological classes. These results agree with the analysis of the 4C sample by McHardy (1979). It has already been shown by Erickson *et al.* (1978), McHardy (1978), Slee and Quinn (1979) and Dagkesamansky *et al.* (1982) that radio sources in powerful X-ray emitting clusters, which are predominantly of morphological class B–M I, have very high spectral indices. Since only six of the 20 radio sources from the present CCA sample are in powerful X-ray clusters it follows that the X-ray luminosity does not determine whether a cluster will contain a steep spectrum source; it is, rather, an indicator.

Summarizing this section, we can state: (i) the spectral index increases systematically towards the cluster centre; (ii) the spectral index does not depend on cluster richness; (iii) the spectral indices of sources in morphological class B–M I clusters are much higher than those in later morphological classes.

5. Radio Powers P_{160} of Cluster Sources

P_{160} and Cluster Richness

Fig. 7a shows the relationship between cluster richness and emitted radio power P_{160} at 160 MHz. As we explained in Section 2, the observed P_{160} have been corrected to a standard redshift of $z = 0.100$ and the median value of the corrected P_{160} was found for each richness class. The K–W ranking test supports the hypothesis that the three samples were drawn from the same population.

P_{160} and Distance from Cluster Centre

The variation of median P_{160} with source distance from the cluster centre is given in Fig. 7b. A K–W ranking test shows that there is a probability $p = 0.03$ that the three samples could have been drawn by chance from the same population. Testing the inner sample against the combination of the two outer samples (bearing in mind that there are three possible ways of choosing such a combination) the difference between the two distributions is significant at $p = 0.03$. Thus, sources within 0.10 Abell radius of cluster centres tend to be more powerful than those at greater distances.

P_{160} and Cluster Morphology

Fig. 7c shows how cluster morphology influences the median radio power. A K–W ranking test supports the hypothesis that the four samples are drawn from the same population. Testing the B–M I/I–II sample against the combination of the remaining three samples (keeping in mind that such a sample can be chosen in six ways), we find that the difference between the two distributions is not significant.

Summarizing this section, we can state: (i) P_{160} is independent of cluster richness; (ii) P_{160} increases by a factor of 1.31 within 0.10 Abell radius of the cluster centre; and (iii) P_{160} is independent of B–M optical morphology.

6. Linear Sizes of Cluster Sources

Linear Size and Distance from Cluster Centre

We have used the method described in Section 2 to correct the individual values of linear size L_{kpc} to the standard redshift of $z = 0.100$; L_{kpc} is the linear size to the 0.1 brightness point of the major axis of the two-dimensional elliptical gaussian giving the best fit to the 160 MHz contour map.

Fig. 8a shows the dependence of linear size on distance from the cluster centre. There *appears* to be a significant increase in size for sources at intermediate distances from the cluster centres, but a K-W ranking test on the three distributions does not support such an interpretation. We conclude that there is no evidence for a change in linear dimension with distance from the cluster centre.

Linear Size and Cluster Richness

Fig. 8b shows that there is no significant variation of linear size with cluster richness. This is supported by a ranking test.

Linear Size and Cluster Morphology

Fig. 8c suggests that sources in clusters of morphological class B-M I may be smaller than those in later classes. Ranking tests on the four distributions do not give these differences much significance.

Summarizing this section, we can state: (i) there is no significant change of linear size with distance from the cluster centre; (ii) linear sizes of radio galaxies do not depend on cluster richness; and (iii) linear size does not depend on cluster morphology.

Table 2. Spectral indices α of cluster and field sources

Type of sample	No. of sources	Mean α	Standard error
(a) Culgoora-3 field sample ^A	127	-0.807	0.017
(b) Present cluster sample	148	-0.864	0.023
(c) Sources within 0.10 Abell radius of cluster centre	57	-0.927	0.035
(d) Sources between 0.20 and 0.40 Abell radius of cluster centre	45	-0.778	0.040
(e) Sources in B-M I clusters	20	-1.033	0.063
(f) Sources in B-M III clusters	62	-0.838	0.040
(g) Sources in <i>both</i> (c) and (e)	10	-1.292	0.095

^A All identified sources in the Culgoora-3 list with $0.02 < z < 0.20$.

7. Comparison of Cluster and Field Sources

The statistical properties of radio galaxies in Abell clusters described in Sections 2-6 should be compared with the corresponding properties of radio galaxies that are not in rich clusters. We have such a sample in the Culgoora-3 list of radio sources (Slee 1977); subsequent analyses of its statistical properties have been made by Slee (1981, 1982) and Slee *et al.* (1982a).

We compare properties that are common to the Culgoora-3 observations and the CCA cluster observations, namely, spectra, radio power P_{160} and maximum linear

dimension L_{kpc} . A legitimate comparison is possible because the data in the two sets of observations were treated in exactly the same manner, i.e. using the same sources of flux data and computer programs to compute radio spectra, P_{160} and L_{kpc} .

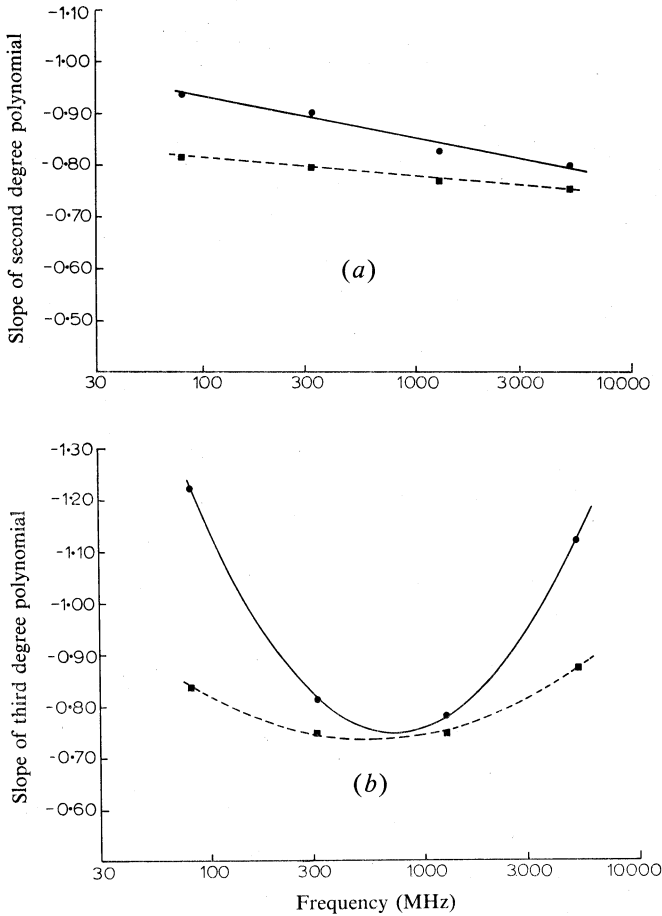


Fig. 9. Median slopes at four frequencies of (a) the second-degree and (b) the third-degree polynomial fits to the $\log S$ - $\log \nu$ data of the CCA cluster sample (circles) and the Culgoora-3 field sample (squares). In (a) the regression lines have slopes of -0.82 for the cluster sample (solid line) and -0.37 for the field sample (dashed line). In (b) the second-degree equations have been least-squares fitted to the points.

Radio Spectra of Cluster and Field Sources

Table 2 lists the mean spectral indices obtained from the Culgoora-3 sample of radio galaxies (Slee 1981) with redshifts in the range $0.02 < z < 0.20$ (the same redshift range as the CCA cluster sample) and various samples of cluster sources. It is clear that, on the whole, cluster sources have significantly steeper spectra than the non-cluster radio galaxies (the standard error of each mean and number of sources allow the significance of the differences to be assessed). However, Table 2 shows that this higher index is due to the high mean indices of sources near cluster centres (entry *c*)

and sources in clusters of morphological type B–M I (entry *e*); the mean indices of sources at distances between 0.20 and 0.40 Abell radius from the cluster centres (entry *d*) and those in B–M III clusters (entry *f*) are not significantly different from the mean index of field sources (entry *a*).

Table 2 suggests that sources within 0.10 Abell radius of the cluster centre in B–M I clusters (entry *g*) may be expected to have particularly steep spectra. An examination of the CCA data shows that 10 sources fulfil this condition, and they have a mean spectral index of -1.292 ± 0.095 ; six of these 10 sources are also in powerful X-ray emitting clusters.

Table 3. Radio powers of cluster and field sources

Type of sample	No. of sources	Median P_{160}^A ($10^{24} \text{ W Hz}^{-1} \text{ sr}^{-1}$)
Culgoora-3 field sample ^B	127	37.3
Present cluster sample	148	10.4
Sources within 0.10 Abell radius of cluster centre	57	11.7
Sources between 0.10 and 0.40 Abell radius of cluster centre	91	8.9

^A Corrected to $z = 0.100$.

^B All identified sources in the Culgoora-3 list with $0.02 < z < 0.20$.

Table 4. Largest linear sizes for cluster and field sources

Type of sample	No. of resolved sources	Median linear size ^A (kpc)
Culgoora-3 field sample ^B	55	675
Present cluster sample	83	542

^A Dimensions of major axis to 0.1 brightness corrected to $z = 0.100$.

^B Resolved sources in Culgoora-3 with $0.02 < z < 0.20$.

Curvature in Spectra of Cluster and Field Sources

Slee *et al.* (1982*a*) and Slee (1982) have already discussed in some detail the second- and third-degree curvature present in the Culgoora-3 sample of field sources. We have applied the same analytical procedure to the CCA cluster sample. Briefly, we fitted second- and third-degree polynomials to the $\log S/\log \nu$ data for the individual sources and found the slopes of the fitted functions at the four standard frequencies 80, 320, 1280 and 5120 MHz. The medians of the distributions of $\partial(\log S)/\partial(\log \nu)$ were plotted and the K–W ranking test applied to the four distributions in order to determine whether they could have come from the same parent population. The K–W ranking test is also applied to the pairs of distributions from the cluster and field samples at *each* of the four frequencies in order to determine the significance of the difference in curvature between the two samples.

Fig. 9*a* shows the results of fitting second-degree polynomials to the spectra of cluster (circles) and field (squares) sources; the field sources are those 127 identified sources in the Culgoora-3 list with redshift $0.02 < z < 0.20$, which is the redshift range of the cluster sample. It is clear from Fig. 9*a* that the average source in both the

cluster and field samples has significant second-degree spectral curvature, but that the curvature is more pronounced in the cluster sample. Ranking tests show that the four distributions in the cluster sample have a probability $p < 0.005$ of having been drawn from the same population, while for the field sample $p \sim 0.05$. Ranking tests on the pairs of distributions at *each* of the four frequencies show that the 80 and 320 MHz pairs are unlikely to have come from the same population ($p < 0.001$); at 1280 and 5280 MHz there is no significant difference between the pairs ($p > 0.1$).

Fig. 9*b* summarizes the results of fitting third-degree polynomials to the spectra of cluster (circles) and field (squares) sources. It is clear that the average source in both samples possesses a significant minimum in spectral slope (i.e. a point of inflexion) at ~ 650 MHz, but that the effect is considerably enhanced in the cluster sample. Ranking tests show that the four distributions in the cluster sample and in the field sample have a probability $p \ll 0.001$ of having been drawn from the same populations. Ranking tests on the pairs of distributions at *each* of the four frequencies show that the 80 and 5120 MHz pairs are very unlikely to have come from the same population ($p \ll 0.001$), while at 320 and 1280 MHz there is no compelling reason to believe that the pairs of distributions have not come from the same population ($p \geq 0.08$). The implications of the second- and third-degree spectral structure that has been described here will be discussed in Section 8.

Radio Power of Cluster and Non-cluster Sources

Table 3 gives the median values of P_{160} for Culgoora-3 field sources and three categories of CCA cluster sources. It is clear that the field radio galaxy is about four times more powerful than the general cluster source; hence, cluster radio galaxies are not particularly powerful examples of the species. It is clear from Table 3 that the power emitted by cluster galaxies increases toward the cluster centre.

Linear Dimensions of Cluster and Field Radio Galaxies

We have already shown in Section 6 that the linear sizes of cluster sources are not dependent on cluster properties. Table 4 compares the median linear sizes of resolved cluster sources with that of the Culgoora-3 sample of field sources. It appears that field sources tend to be some 130 kpc larger than sources in clusters; a K-W ranking test on the two distributions shows that the difference is significant at the 0.05 level.

It could be argued that the difference between the median linear sizes is due to the possibility that linear size depends on power output (see e.g. Fanaroff and Riley 1974), and indeed Table 3 shows that the field sources are about four times more powerful than the cluster sources. In order to check this possibility we have computed the power-law regression of P_{160} (corrected to $z = 0.100$) on L_{kpc} (corrected to $z = 0.100$) for both the Culgoora-3 and cluster samples. No significant relationship was found between L_{kpc} and P_{160} . We must therefore conclude that the difference in median linear dimensions of the two samples is not due to differences in power output and that cluster membership does significantly reduce the source dimensions.

Luminosity Functions for Cluster and Field Sources

We have computed luminosity functions for the cluster and Culgoora-3 field samples using the maximum-volume method of Schmidt (1968). The computations were made with an Einstein-de Sitter cosmology and $H_0 = 50 \text{ km s}^{-1} \text{ Mpc}^{-1}$. The luminosity functions are tabulated in Table 5 and plotted in Fig. 10.

It is clear from Fig. 10 that the luminosity function of field sources lies consistently above that for the cluster sources and on log-log scales the two functions have similar slopes; the fact that most of the data can be well fitted by straight lines is consistent with a power-law form for the luminosity functions (Sholomitskii 1968).

Table 5. Luminosity functions
Units of P_{160} are $\text{W Hz}^{-1} \text{sr}^{-1}$; ρ sources Mpc^{-3}

$\log_{10}\langle P_{160}\rangle$	No. of sources	Mean red-shift $\langle z \rangle$	$\log_{10} \rho^{\text{A}}$	Error in $\log_{10} \rho^{\text{B}}$
<i>Culgoora-3 field sample</i>				
24.50	8	0.036	-6.93	+0.13
24.77	22	0.041	-6.88	-0.19
25.06	20	0.055	-7.32	+0.08
25.39	14	0.071	-7.93	-0.10
25.64	21	0.102	-8.08	+0.09
25.96	17	0.131	-8.60	-0.11
26.30	9	0.149	-9.36	+0.10
26.92	5	0.143	-10.99	-0.14
<i>CCA cluster sample</i>				
24.04	5	0.026	-7.23	+0.09
24.50	14	0.052	-7.17	-0.12
24.74	21	0.063	-7.34	+0.10
25.09	29	0.099	-7.66	-0.13
25.34	29	0.127	-7.99	+0.09
25.64	11	0.141	-8.83	-0.11
26.03	2	0.171	-10.11	+0.07
				-0.09
				+0.07
				-0.09
				+0.11
				-0.16
				+0.23
				-0.53

^A In computing ρ the Culgoora-3 sample was assumed to be complete to $S_{160} \geq 4.5$ Jy (Slee 1982) and the CCA cluster sample complete to $S_{160} \geq 2.0$ Jy.

^B Error is derived from the number of sources in each range of P_{160} assuming a Poisson distribution for which $\sigma = \rho/\sqrt{n}$.

The sudden flattening of both functions at their low luminosity ends is probably due to a selection effect; although we believe that the cluster and Culgoora-3 samples are complete to flux levels of 2.0 and 4.5 Jy per beam respectively (sources of lower S_{160} have been excluded from the computations of these functions), it is likely that some of the more extended sources in the nearest clusters with total fluxes above these limits are escaping detection because of their reduced surface brightness. We have ignored these disparate values and made a least-squares fit of straight lines to the remainder. In logarithmic form the regression equations are

$$\begin{aligned} \log \rho &= 38.82 - 1.86(\pm 0.29) \log P_{160}, & \text{for CCA cluster sample;} \\ &= 38.81 - 1.84(\pm 0.14) \log P_{160}, & \text{for Culgoora-3 field sample,} \end{aligned}$$

where ρ is the source density (Mpc^{-3}) and P_{160} the emitted 160 MHz power ($\text{W Hz}^{-1} \text{sr}^{-1}$).

In view of the standard errors in the slopes of these equations, the data are consistent with identical power-law exponents for the luminosity functions of cluster and field sources.

The average ratio of source densities in the two samples over the common luminosity range is 4.4, indicating that only $\sim 20\%$ of all radio galaxies with $0.02 \leq z \leq 0.20$ are associated with rich clusters. This conclusion agrees with those of Mills and Hoskins (1977) and McHardy (1979).

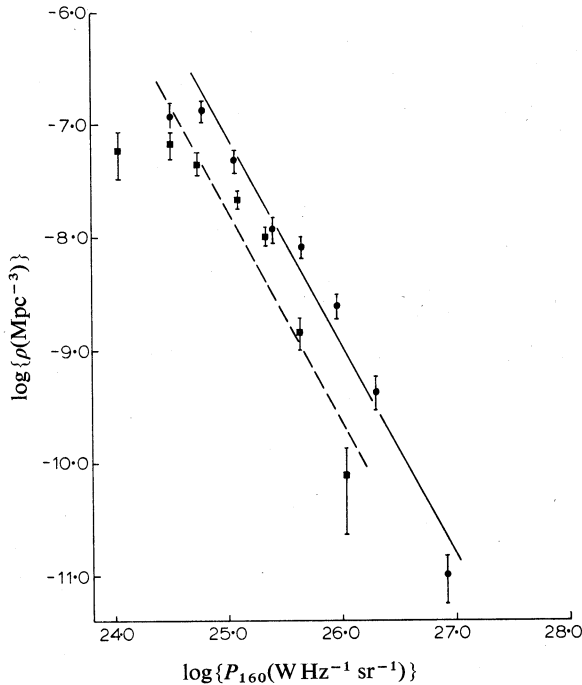


Fig. 10. Luminosity functions for the Culgoora-3 field sample (solid line and circles) and the CCA cluster sample (dashed line and squares). The slopes of the regression lines (exponents of power-law luminosity functions) are $-1.84(\pm 0.14)$ for the Culgoora-3 sample and $-1.86(\pm 0.29)$ for the cluster sample.

8. Interpretation and Discussion

The properties of radio sources in clusters should reflect the influence on the formation and subsequent evolution of radio galaxies of the physical properties of the clusters (for example, gravitational field, magnetic field, gas density and temperature).

The optically identified radio galaxies of high power output, whether in the general field or in clusters, are usually associated with intrinsically bright elliptical, D and cD galaxies (Colla *et al.* 1975). The result that B-M I clusters are about three times as likely to contain a radio source as other morphological classes (Section 3 and Fig. 4) is then naturally explained by the fact that B-M I clusters *always* contain a very luminous centrally located cD galaxy. However, our measurements of P_{160} (Section 5) show that radio sources in B-M I clusters are not generally more powerful than those in clusters of other morphological classes; this suggests that the cD, D and giant ellipticals that *sometimes* occur in the later classes are as luminous as the centrally located cD galaxies in B-M I clusters. The fact that P_{160} is highest for centrally located radio galaxies (Section 5 and Fig. 7*b*), irrespective of cluster optical morphology, is consistent with such an interpretation. The result that cluster richness does

not influence the P_{160} of a radio galaxy (Section 5 and Fig. 7a) is expected if the radio and optical luminosities of elliptical galaxies are well correlated, as found by Colla *et al.* (1975); a detailed study of the brightest elliptical galaxies in clusters by Oemler (1976) showed that the brightness of the elliptical core is only a very slowly increasing function of cluster richness.

The high spectral indices of radio sources in clusters, especially those near cluster centres and in B–M I clusters, is most likely a consequence of the effects of gas in the central region. The emission of powerful X-rays with an apparently thermal spectrum from a considerable number of clusters has been attributed to a hot (10^8 K) intra-cluster gas with an electron density of $\sim 10^{-3} \text{ cm}^{-3}$ at the cluster centre (see e.g. McHardy 1978). Such a gas within and surrounding a radio galaxy may conceivably retard the expansion of the relativistic electrons and thus allow the source to retain its identity for a longer interval than is the case for a field radio galaxy. This would eventually result in a steepening of the radio spectrum caused by synchrotron radiation losses. Our results (Section 4 and Table 2) support this hypothesis and further suggest that the steepening of the radio spectrum provides a more sensitive method of detecting this gas than the use of existing X-ray telescopes: a significant steepening of the spectrum is detected in most radio sources near cluster centres (Fig. 6a), whether or not the cluster is a strong X-ray emitter, although the latter do contain the steepest spectrum sources (Slee and Quinn 1979). The observational evidence from Oemler (1976) is that cD and other types of the brightest elliptical cluster galaxies appear to be very bright but otherwise normal ellipticals on which very diffuse extended envelopes are superimposed. The dominant galaxies in B–M I clusters (cD galaxies) always have extensive envelopes, even in clusters of richness class O, whereas the brightest cluster galaxies in later B–M classes have gaseous envelopes whose luminosities and dimensions increase with cluster richness. The optical evidence suggests that if the source confinement hypothesis is correct then there may be an increase of spectral index with cluster richness, at least for the B–M II, II–III and III clusters. Our results (Section 4 and Fig. 6b) do not demonstrate a convincing relationship between spectral index and richness; the same negative result is obtained if only sources in B–M II, II–III and III clusters are considered. To retain the source confinement hypothesis, one must postulate that there is considerable gas surrounding giant ellipticals in even the poorest clusters, despite the fact that its presence is not always detected by optical or X-ray observations.

The relative linear sizes of sources in clusters and field sources has been the subject of disagreement among several authors; one would expect from the source confinement hypothesis that the sources in clusters would be smaller. De Young (1972) concluded that the cluster sources were smaller, while Hooley (1974), Lari and Perola (1978) and McHardy (1978) found no significant difference in maximum dimensions. Our conclusion (Section 7 and Table 4) that sources in clusters are more compact than field sources takes into account the possible dependence of linear size on radio power and redshift; the latter dependence (imposed on the data by the angular size limit of our observations) is almost certainly present in earlier studies, although the authors did not specifically mention that they have corrected their data for the effect. If our result is valid, then the absence of a dependence of linear size on cluster richness and cluster morphology (Section 6) is consistent with our conclusions from a study of spectral index, i.e. that all clusters of whatever richness and/or B–M class contain enough gas to retard the expansion of their radio galaxies.

The luminosity functions for cluster and field sources (Section 7 and Fig. 10) show that $\sim 20\%$ of radio galaxies with $10^{24.1} < P_{160} < 10^{25.6} \text{ W Hz}^{-1} \text{ sr}^{-1}$ lie in Abell clusters, whereas only $\sim 12\%$ of galaxies are found in such clusters (Peebles 1974). The apparent discrepancy is explained by the strong dependence of radio power on the absolute optical magnitude of a galaxy (Colla *et al.* 1975) and the fact that the most luminous E, D and cD galaxies occur preferentially in clusters (Oemler 1976). In addition, the absence of a strong correlation between the optical luminosity of the brightest galaxy and the cluster richness explains why powerful radio sources are just as likely to be found in poor clusters as in rich clusters (Section 3).

The presence of significant second-degree curvature in the $\log S - \log \nu$ data of sources in both the cluster and field samples (Fig. 9a) could be interpreted as the result of adding the spectra of unresolved components, some with steeper power-law spectra than others. The model proposed by Kellermann (1966) of a single source with repeated injections of hard relativistic electrons accompanied by evolution due to synchrotron and Compton losses would lead to second-degree curvature of the opposite sign; such a model is more consistent with the observed spectra of field galaxies of high redshift and unidentified (blank-field) sources (Slee 1982). It is clear from Fig. 9a that, besides the fact that the spectral slopes of the cluster sample are systematically higher than those in the field sample (as would be expected from the first-degree analysis), the rate of change of slope frequency is also much higher for the cluster sample. In a two-component model this would be caused by relatively more power in the steeper spectrum component and/or by a larger contrast in the power-law spectra of the components.

A more interesting discovery is the third-degree curvature in the $\log S - \log \nu$ data from both the cluster and field samples (Fig. 9b). Such spectral structure could only be produced in the multi-component model by combining 'normal' power-law spectra with spectra having low-frequency cut-offs, such as those described by Kellermann and Pauliny-Toth (1969). However, most of the well-known examples of such spectra occur in QSOs, whereas our results are concerned with radio galaxies, whose linear dimensions (emitting most of the power in the frequency range of our spectra) are generally too large to give rise to self-absorbed spectra of the type seen in QSOs.

An alternative evolutionary interpretation of the third-degree structure, first advanced by Slee (1982), is based on the apparent dependence on redshift of the depth of minimum in spectral slope at $\sim 650 \text{ MHz}$. It is applicable to substantially single sources (i.e. sources with one dominant power-law spectrum). In the complete Culgoora-3 sample of identified radio galaxies Slee (1982) showed that the inflexion point became noticeable only for radio galaxies with redshifts below $z \approx 0.1$ and was most pronounced at the lowest redshifts. If we interpret redshift in terms of 'look-back time', this behaviour indicates that we are witnessing the development of an evolutionary influence on the radio spectrum.

In the CCA sample of sources in clusters the minimum is already very pronounced for galaxies with $\langle z \rangle = 0.095$; in the Culgoora-3 sample of identified field sources with redshifts in the same range as the cluster sample ($\langle z \rangle = 0.082$) the spectral index minimum is present but is not as pronounced. The main difference between the two sets of spectra is due to the cluster sources having much steeper spectra at both ends of the radio spectrum. If we postulate that the departure of a radio spectrum from a power-law form is due only to synchrotron and Compton losses combined with repeated injections of fresh relativistic electrons (Kellermann 1966), then

spectra with inflexion points of the kind seen in Fig. 9b are not predicted. A possible additional important evolutionary process could be the diffusion of relativistic electrons in momentum space. This could be due to some as yet unidentified scattering mechanism connected with the presence of a hot, ambient gas in the radio galaxy; in the cluster sample there is indeed good independent evidence from X-ray observations for the presence of a relatively dense, high-temperature electron gas. Theoretical computations of the effects of diffusion on relativistic electron energy distributions by Kontorovich and Kochanov (1980) do indeed predict complex spectral structure for some models. It would be interesting to combine diffusion and synchrotron and Compton losses with repeated injections (or re-accelerations) in a theoretical treatment of a realistic model for a radio galaxy. The resulting predicted spectra at different epochs could profitably be compared with the observed spectra of radio galaxies of differing redshifts.

Acknowledgments

We thank Dr Alan E. Wright for his critical reading of the manuscript and his many suggestions for its improvement.

Reference

- Abell, G. O. (1958). *Astrophys. J. Suppl.* **3**, 211.
 Colla, G., *et al.* (1975). *Astron. Astrophys.* **38**, 209.
 Dagkesamansky, R. D., Gubanov, A. G., Kuzmin, A. D., and Slee, O. B. (1982). *Mon. Not. R. Astron. Soc.* **200**, 971.
 de Young, D. S. (1972). *Astrophys. J.* **173**, L7.
 Erickson, W. C., Matthews, T. A., and Viner, M. R. (1978). *Astrophys. J.* **222**, 761.
 Fanaroff, B. L., and Riley, J. M. (1974). *Mon. Not. R. Astron. Soc.* **167**, 31P.
 Gower, J. F. R. (1966). *Mon. Not. R. Astron. Soc.* **133**, 151.
 Hooley, A. (1974). *Mon. Not. R. Astron. Soc.* **166**, 259.
 Hughes, A., and Grawoig, D. (1971). 'Statistics: A Foundation for Analysis' (Addison-Wesley: Cambridge, Mass.).
 Kellermann, K. I. (1966). *Astrophys. J.* **146**, 621.
 Kellermann, K. I., and Pauliny-Toth, I. I. K. (1969). *Astrophys. J.* **155**, L71.
 Komesaroff, M. M., Slee, O. B., and Higgins, C. S. (1968). *Proc. Astron. Soc. Aust.* **1**, 102.
 Kontorovich, V. M., and Kochanov, A. E. (1980). *Astrophys. Space Sci.* **71**, 265.
 Lari, C., and Perola, G. C. (1978). In 'The Large-scale Structure of the Universe' (Proc. IAU Symp. No. 79) (Eds M. S. Longair and J. Einasto), p. 137 (Reidel: Dordrecht).
 Leir, A. A., and van den Bergh, S. (1977). *Astrophys. J. Suppl. Ser.* **34**, 381.
 McHardy, I. (1978). *Mon. Not. R. Astron. Soc.* **184**, 783.
 McHardy, I. (1979). *Mon. Not. R. Astron. Soc.* **188**, 495.
 Mills, B. Y., and Hoskins, D. G. (1977). *Aust. J. Phys.* **30**, 509.
 Oemler, A., Jr (1976). *Astrophys. J.* **209**, 693.
 Owen, F. N. (1974). *Astron. J.* **79**, 427.
 Owen, F. N. (1975). *Astron. J.* **80**, 263.
 Peebles, P. J. E. (1974). *Astrophys. J. Suppl.* **28**, 37.
 Pilkington, J. D. H. (1964). *Mon. Not. R. Astron. Soc.* **128**, 103.
 Schmidt, M. (1968). *Astrophys. J.* **151**, 393.
 Sholomitskii, G. B. (1968). *Sov. Astron.* **11**, 756.
 Slee, O. B. (1977). *Aust. J. Phys. Astrophys. Suppl.* No. 43.
 Slee, O. B. (1981). *Proc. Astron. Soc. Aust.* **4**, 184.
 Slee, O. B. (1982). In 'Extragalactic Radio Sources' (Proc. IAU Symp. No. 97) (Eds D. S. Heeschen and C. M. Wade), p. 35 (Reidel: Dordrecht).
 Slee, O. B., and Quinn, P. J. (1979). *Proc. Astron. Soc. Aust.* **3**, 332.

- Slee, O. B., Siegman, B. C., and Mulhall, P. (1982a). *Proc. Astron. Soc. Aust.* **4**, 278.
Slee, O. B., Wilson, I. R. G., and Siegman, B. C. (1982b). *Proc. Astron. Soc. Aust.* **4**, 431.
Wall, J. V., Shimmins, A. J., and Merkelijn, J. K. (1971). *Aust. J. Phys. Astrophys. Suppl.* No. 19.
Wills, D. (1966). *Observatory* **86**, 140.

Manuscript received 6 August, accepted 6 October 1982